https://doi.org/10.52326/ic-ecco.2022/EL.04

Algorithms of Overmodulation Regulation of Neutral Clamped Inverters for Photovoltaics

Valentin Oleschuk, ORCID: 0000-0002-7413-4867
Institute of Power Engineering
Str. Academiei 5, Chisinau, MD-2028, Republic of Moldova

***Abstract*—This manuscript presents results of study and research of synchronous adjustment in the overmodulation control zone of three neutral-clamped inverters (NCIs) of the specific configuration of three-phase grid-connected photovoltaic system. It has been proved, that the corresponding modification of techniques and algorithms of pulsewidth modulation (PWM) for control of NCIs, assure symmetry and advanced harmonic composition of inverter-side winding voltage of multi-winding power transformer, thereby helping to reduce losses in windings of the transformer, and to improve the efficiency of photovoltaic installations.**

***Keywords*—control, modulation, converter, photovoltaics, voltage, harmonics, spectrum**

I. Introduction

New structures and topologies of multi-level and multi-phase converters of the parameters of electrical energy, with the help of which rational and economical modes of operation of systems of various functional purposes are provided, are increasingly being used in the field of electric drives, electric transport, and renewable sources of electric energy [1] – [4].

Photovoltaic systems are ones of the most common renewable energy installations [5] - [6]. Currently, there are a large number of structures of PV installations of transformer-based and transformer-less types [7] - [8]. In this case, various configurations of inverters can be used in PV systems [9] – [11].

The efficiency of the functioning of inverter-based PV systems is highly dependent on the methods and techniques of control and pulsewidth modulation (PWM) used to adjustment of inverters of the corresponding installations [12] - [14]. To provide improved spectral composition of the basic voltages of PV system with three neutral clamped inverters (NCIs) operating in the zone of overmodulation, specialized PWM algorithms for adjustment of NCIs have been elaborated and investigated in this paper.

II. Structure of Three-NCI-Based PV System

Recently, inverter-based grid-tied photovoltaic installation with three two-level inverters and with specific interconnection between outputs of PWM inverters and windings of power transformer has been described (Fig. 1 [9], [10]).

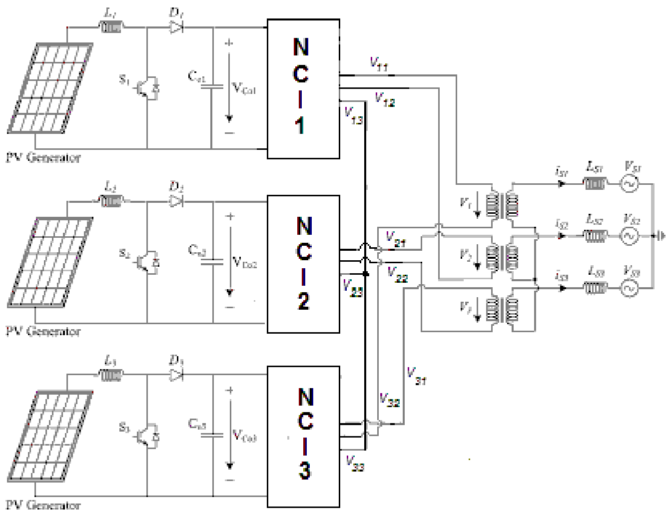

Figure 1. Basic power circuits of PV system with three Neutral Clamped Inverters (**NCI1** – **NCI3)** with special interconnections with power transformer.

https://doi.org/10.52326/ic-ecco.2022/EL.04

Fig. 1 presents slightly modified topology of the PV installation [9] based on three neutral clamped inverters (**NCI1**, **NCI2**, and **NCI3**), polar voltages of which $V_{11} - V_{32}$ are applied specifically to the corresponding windings of power transformer. This structure of PV system assures the increase of the maximum voltage applied to the multi-winding transformer (in comparison with two-inverter-based PV systems), reducing its weight and volume [9].

III. Switching Scheme of Neutral Clamped Inverters

Fig. 2,a shows structure of power circuits of NCI, Fig. 2,b presents basic voltage vectors **V1** ÷ **V7** (seven vectors, marked by the big arrows) of each NCI. Control and PWM scheme is based in this case on the using of six basic vectors (large vectors **V1** ÷ **V6),** and of the zero vector **V7**, assures providing minimization of value of common-mode voltage in power conversion systems with NCIs [8]. As an additional fact, it assures also to provide balanced neutral-point voltage of each NCI due to the fact that the presented **V1** ÷ **V7** vectors of voltage of diode clamped inverters do not have influence at the fluctuation of the neutral point voltage because the neutral-point **0** in this case is not connected to the NCI output [15].

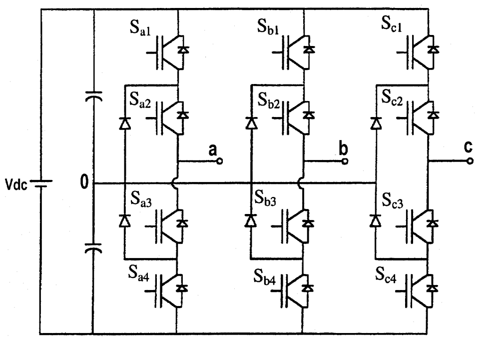

a)

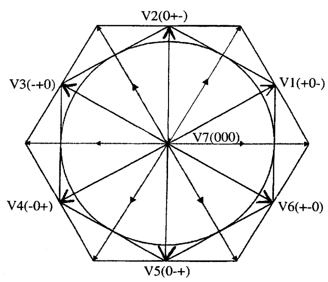

b)

Figure 2. Structure of power circuits of diode clamped inverter (a), and its basic voltage vectors **V1**÷**V7** (b).

IV. Features of Synchronous Control of NCIs of PV Installation in the Overmodulation Zone

To insure symmetry of the output voltage of NCI, modified techniques of synchronous space-vector PWM can be disseminated for regulation of neutral clamped inverters of the analyzed photovoltaic installation [4], [13]. Fig. 3 presents (inside the clock-time 0^0 - 60^0) diagrams of switching state sequence, and pole and line voltages of NCI controlled by the technique of continuous synchronous PWM, assuring symmetry of NCI output voltage over the whole adjustment range [12].

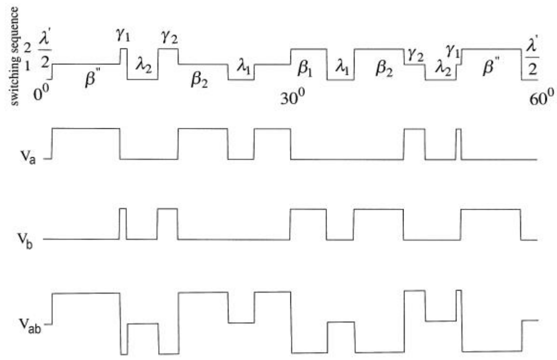

Figure 3. Switching sequence, and basic voltages V_a, V_b,, V_{ab} of NCI with synchronous PWM inside the clock-time 0^0 - 60^0.

Control of inverters of PV installations in the zone of the high and the highest coefficients of modulation *m* of inverters (in the zone of overmodulation, when *m>0.907*), has some specific features. Boundary values of two coefficients of modulation of inverters for the case of conventional two-stage adjustment in the zone of overmodulation are correspondingly equal to $m_{ov1} = 0.907$ and $m_{ov2} = 0.952$ [14] ($m_{\max} = 1$ in this case). Particularly, basic control dependences of voltage source inverters with synchronous PWM for determination of parameters of control signals include two specialized indices of overmodulation $K_{ov1} = [1-(m-m_{ov1})/(m_{ov2}-m_{ov1})]$ and $K_{ov2} = [1-(m-m_{ov2})/(1-m_{ov2})]$:

If *0.952>m>0.907*:

$$\beta_1 = \tau \qquad (1)$$

$$\beta_j = \beta_1 \cos[(j-1)\tau K_{ov1}] \qquad (2)$$

$$\gamma_j = \beta_{n-j+1}\{0.75 - 0.55\tan[(n-j)\tau]\} \qquad (3)$$

$$\lambda_j = \tau - (\beta_j + \beta_{j+1})/2 \qquad (4)$$

If *1>m>0.952*:

$$\beta_1 = \tau \tag{5}$$

$$\beta_j = \beta_1 \cos[(j-1)\tau K_{ov2}] \tag{6}$$

$$\gamma_j = \beta_{n-j+1}\{0.75 - 0.55\tan[(n-j)\tau]\}K_{ov2}, \tag{7}$$

where m – index of modulation of NCI, $\beta_1 - \beta_j$ - (see Fig. 3) duration of total active switching state during sub-cycle, γ_j - minor part of duration of active switching state, λ_j - duration of notches, τ - switching sub-cycle.

V. Operation of Three NCIs of PV Installation in the Zone of Overmodulation

A. *System Control at the First Stage of the Over-modulation Zone of Neutral Clamped Inverters*

Winding voltages V_1, V_2, V_3 of inverter-side windings of multi-winding power transformer of photovoltaic installation (Fig. 1) can be determined as functions of the corresponding pole voltages of three NCIs [9]:

$$V_1 = V_{11} - V_{13} - V_{32} + V_{33} \tag{8}$$

$$V_2 = V_{21} - V_{23} - V_{12} + V_{13} \tag{9}$$

$$V_3 = V_{31} - V_{33} - V_{22} + V_{23} \tag{10}$$

In accordance with the used PWM strategy, control signals of three NCIs are shifted by 120^0, and additional mutual phase shift between control signals of inverters is equal to 1/3 of the width of switching sub-cycle.

During the first control part of operation of NCIs of PV installation in the zone of overmodulation (modulation index m of inverters is $0.952>m>0.907$ in this sub-zone), control and modulation process is characterized by a smooth quasi-linear enlargement of duration of total active control signals of inverters (β - parameter in (2)) until its width will be equal to duration of switching interval τ [14]. Simultaneously, smooth decrease of duration of all notches λ (4) until close to zero value is observed in this control sub-zone.

Fig. 4 – Fig. 5 present results of simulation of PV installation with NCIs controlled by algorithms of synchronous discontinuous PWM (PWMD), described in [8], and show, in the relative scale, pole voltages V_{11}, V_{12} and V_{13} of the first NCI, line voltages of NCI1 and NCI2 ((V_{12} - V_{13}) and (V_{21} - V_{23})), and winding voltage V_2 of power transformer. It presents also (Fig. 5) spectra of the line (V_{21} - V_{23}) voltage, and of the winding voltage V_2. Fig. 6 – Fig. 7 present the corresponding diagrams for system controlled by algorithm of "direct-direct" PWM (PWMDD, [8]). The fundamental frequency of system is equal to $F = 50$ *Hz*, switching frequency of NCIs is equal to $F_s = 1000$ *Hz*, and its modulation index $m = 0.945$.

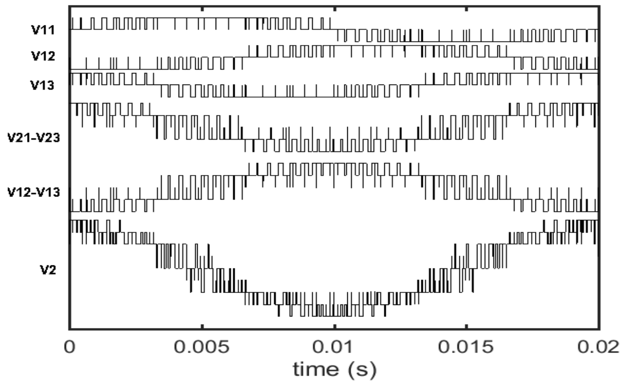

Figure 4. Pole voltages V_{11}, V_{12} and V_{13}, line voltages, and winding voltage V_2 of PV system adjusted by the scheme of PWMD ($m = 0.945$).

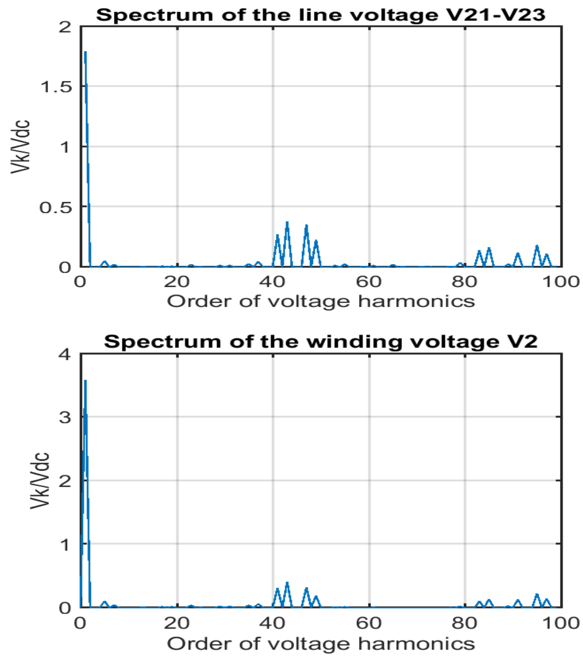

Figure 5. Harmonic composition of voltages of PV installation with discontinuous PWM (PWMD, $F = 50$ *Hz*, $F_s = 1000$ *Hz*, $m = 0.945$).

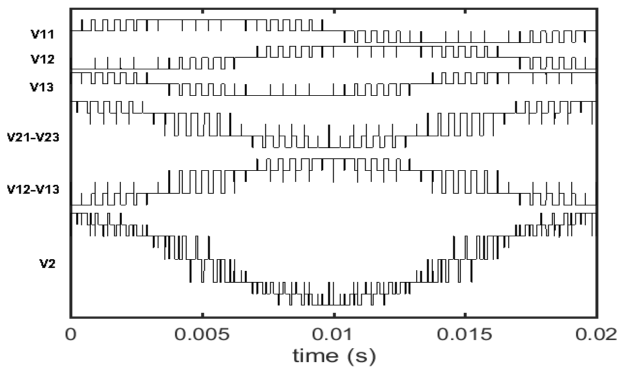

Figure 6. Pole voltages V_{11}, V_{12} and V_{13}, line voltages, and winding voltage V_2 of PV system adjusted by the scheme of PWMDD ($m = 0.945$).

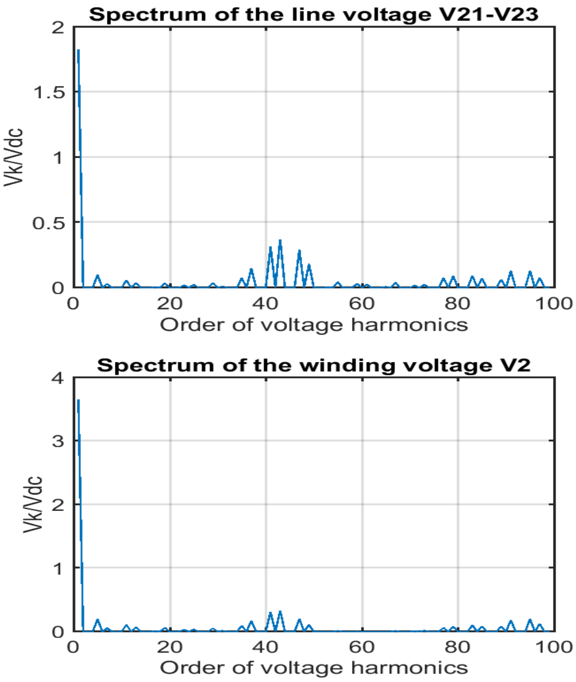

Figure 7. Harmonic composition of voltages of PV installation with 'direct-direct' PWM (PWMDD, *F = 50 Hz*, F_s *= 1000 Hz*, *m = 0.945*).

B. *System Control at the Second Stage of the Overmodulation Zone of NCIs*

During the second stage of operation of neutral clamped inverters of transformer-based grid-tied PV installation in the zone of overmodulation (modulation index *m* of NCIs is $1>m>0.952$ in this sub-zone), control and modulation process is characterized by a smooth reduction of the widths of the γ -parameters (7) until close to zero value in regime characterized by the maximum value of index of modulation of NCIs ($m = 1$) [8].

In order to illustrate processes of control and pulsewidth modulation in PV system with three NCIs (adjusted by the two basic schemes (PWMD and PWMDD) of synchronous PWM for NCIs) during the second sub-zone of overmodulation control diapason, Fig. 8 – Fig. 11 present basic voltage waveforms of the analazyed photovoltaic installation, and also spectral characteristics of the line voltage (V_{21} - V_{23}) and winding voltage V_2.

Fig. 8 – Fig. 9 show the corresponding diagrams for PV system with NCIs, adjusted by the scheme of discontinuous synchronous modulation (PWMD), Fig. 10 – Fig. 11 present the corresponding diagrams for PV installation with NCIs, regulated by techniques of 'direct-direct' synchronous PWM (PWMDD). Coefficient of modulation of NCIs in this case is equal to $m=0.985$, average switching frequency of power switches of neutral clamped inverters is equal to *1000 Hz*.

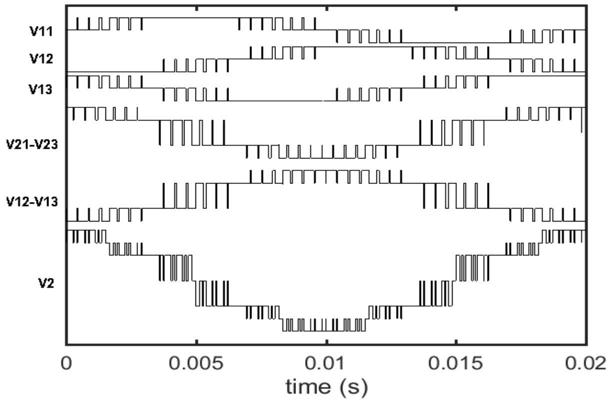

Figure 8. Pole voltages V_{11}, V_{12} and V_{13}, line voltages, and winding voltage V_2 of PV system adjusted by the scheme of PWMD ($m = 0.985$).

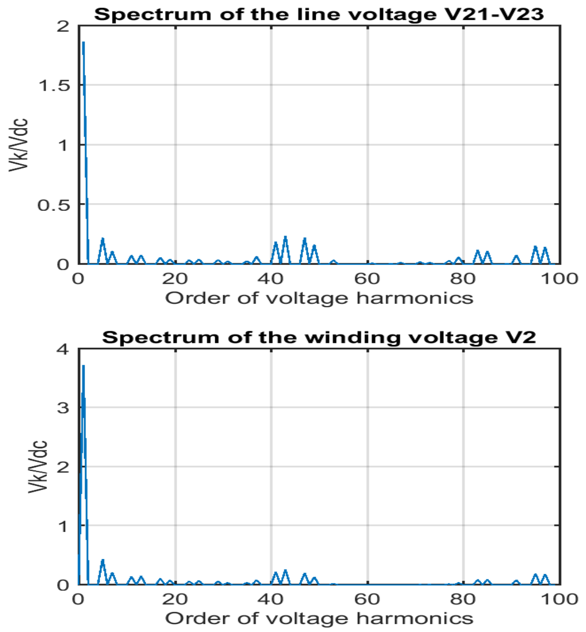

Figure 9. Harmonic composition of voltages of PV installation with discontinuous PWM (PWMD, *F = 50 Hz*, F_s *= 1000 Hz*, *m = 0.985*).

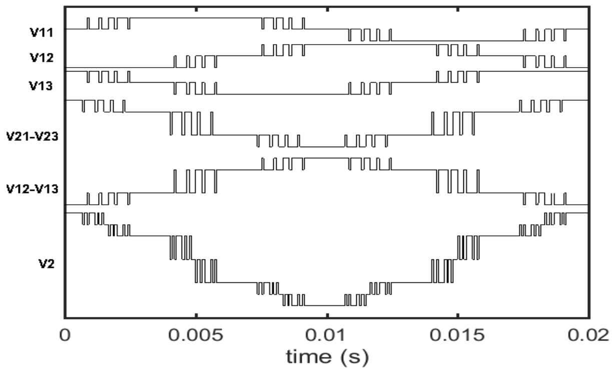

Figure 10. Pole voltages V_{11}, V_{12} and V_{13}, line voltages, and winding voltage V_2 of PV system adjusted by the scheme of PWMDD ($m = 0.985$).

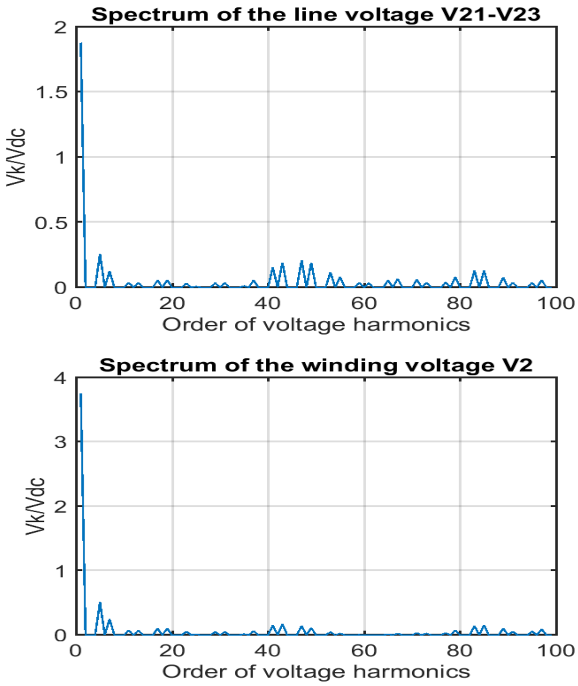

Figure 11. Harmonic composition of voltages of PV installation with 'direct-direct' PWM (PWMDD, $F = 50$ Hz, $F_s = 1000$ Hz, $m = 0.985$).

Shown in Fig. 4 - Fig. 11 diagrams and spectrograms illustrate the fact that in the analyzed three-NCI-based PV installation, modified techniques and algorithms of synchronous space-vector modulation, disseminated for regulation of three neutral clamped inverters, can successfully assure the symmetry and advanced harmonic composition of the winding voltage of multi-winding power transformer (without even-order harmonics and subharmonics in spectra of the winding voltage) during control of NCIs in the zone of overmodulation.

So, improved harmonic composition of the winding voltage of transformer of grid-tied PV system insures to decrease losses in the inverter-side windings of multi-winding power transformer.

Total Harmonic Distortion (*THD*) factor is an important indicator for study and comparison of integral spectral composition of winding voltage V_2 of the analyzed PV installation with triple NCIs, adjusted by algorithms of synchronous PWMD and PWMDD, with switching frequency of power switchs of neutral clamped inverters equal to *1000 Hz*, determinate (and presented in Fig. 12) for the case of two values of the maximum number of the calculated low order harmonics (*k*-th harmonics) – $k = 100$, and $k = 1000$:

$$THD = (1/V_{2_1})\sqrt{\sum_{k=2}^{100} V_{2_k}^2} \tag{11}$$

$$THD = (1/V_{2_1})\sqrt{\sum_{k=2}^{1000} V_{2_k}^2} \tag{12}$$

The presented in Fig. 12 diagram shows a relatively big dependence of the value of the *THD* factor of the winding voltage on number of low order voltage harmonics, taking into account during determining *THD*. But for the both cases of determining of the *THD* factor, presented in Fig. 12 ($k = 100$ and $k = 1000$), better values of *THD* factor can be assured by the using of algorithms of the "direct-direct" scheme of synchronous pulsewidth modulation for specific control of three neutral clamped inverters of the analyzed PV installation in the zone of overmodulation.

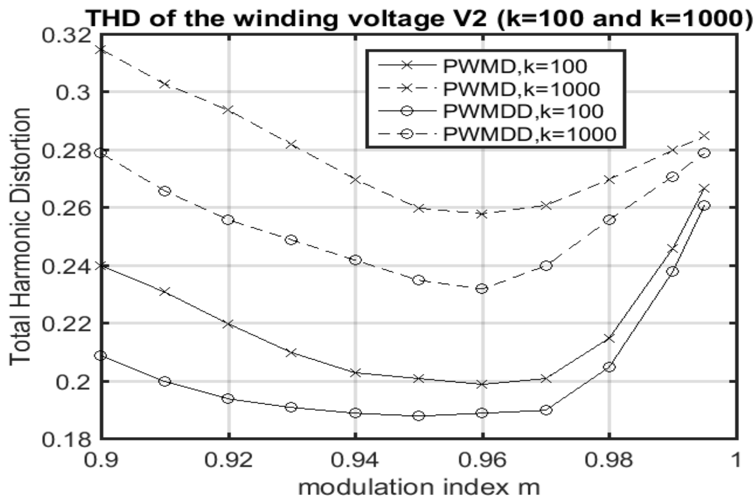

Figure 12. *Total Harmonic Distortion (THD)* factor of the winding voltage V_2 of PV installation based on triple NCIs.

https://doi.org/10.52326/ic-ecco.2022/EL.04

CONCLUSION

It is shown that the modified control scheme and algorithms of synchronous space-vector PWM can be successfully used to control of three neutral clamped inverters of a transformer-based PV installation with a special interconnection between windings of the power transformer with output circuits of the inverters, ensuring the symmetry of the voltage waveforms on the inverter-side windings of the power transformer under specific operating conditions of the inverter block of the system in the overmodulation zone.

Presented in Figs. 5, 7, 9, and 11 characteristics of the spectral composition of the line voltage of inverters, regulated on the basis of modified algorithms of synchronous space-vector PWM, and of the resulting winding voltage of the power transformer, emphasize the fact that there are no even order harmonics and subharmonics (of the fundamental frequency of system) in spectra of these basic voltages over the entire range of two-stage regulation of inverters in the overmodulation control zone, including cases of fluctuation of the operating frequency of the PV system connected with a three-phase grid.

On the basis of a comparative analysis of the integral spectral characteristics of the base voltages in the system, it was determined that improved (reduced) values of the distortion factor of the resulting winding voltage of power transformer are provided by regulating neutral clamped inverters on the base of modified algorithms of the “direct-direct” scheme of synchronous PWM.

Improving the harmonic composition of the winding voltage of the power transformer of the analyzed system makes it possible to reduce losses in the transformer, thereby contributing to an increase in the efficiency of the functioning of three-phase transformer-based photo-voltaic installations.

REFERENCES

[1] B.K. Bose, “Power electronics, smart grid, and renewable energy systems,” *Proceedings of the IEEE,* vol. 105, no. 11, pp. 2011-2018, 2017.

[2] M. Malinowski, K. Gopakumar, J. Rodriguez, and M.A. Pérez, “A survey on cascaded multilevel inverters,” *IEEE Trans. Ind. Electron.*, vol. 57, no.7, pp. 2197-2206, 2010.

[3] P. Sankeevikumar, M.S. Bhaskar, P.K. Maroti, F. Blaabjerg, P. Siano, and V. Oleschuk, “Hextuple-inverter configuration for multilevel nine-phase symmetrical open-winding converter,” *Proc. of IEEE Int’l Conf. on Power Electronics, Intelligent Control and Energy Systems (ICPEICES’2016),* 6 p., 2016.

[4] V. Oleschuk, M. Tirsu, and I. Vasiliev, “Multilevel power electronic systems adjusted by algorithms of multi-zone space-vector modulation: A survey,” *Proc. of IEEE Int’l Conf. on Development and Application Systems (DAS’2022)*, pp. 124-131, 2022.

[5] G. Grandi, C. Rossi, D. Ostojic, and D. Casadei, “A new multilevel conversion structure for grid-connected PV applications,” *IEEE Trans. Ind. Electron.*, vol. 56, no. 11, pp. 4416–4426, 2009.

[6] G.K. Singh, “Solar power generation by PV (photovoltaic) technology: a review,” *Energy*, vol. 53, pp. 1–13, 2013.

[7] C. Cecati, F. Ciancetta, P. Siano, ‘A multilevel inverter for photovoltaic systems with fuzzy logic control,” *IEEE Trans. Ind. Electron*., vol. 57, no. 12, pp. 4115–4125, 2010.

[8] V. Oleschuk, G. Griva, and F. Spertino, “Dual neutral-point-clamped converters with synchronized PWM for photovoltaic installations,” *International Review of Electrical Engineering*, vol. 5, no. 1, pp. 123-131, 2010.

[9] V.F. Pires, A. Cordeiro, D. Foito, and J.F. Silva, “Three-phase multilevel inverter for grid-connected distributed photovoltaic systems based in three three-phase two-level inverters,” *Solar Energy*, vol. 174, pp. 1026-1034, 2018.

[10] V. Oleschuk, “Grid-connected PV system employing three inverters regulated by synchronous scheme of PWM,” *Technical Electrodynamics,* no. 5, pp. 23-28, 2022.

[11] N.A. Rahim, K. Chaniago, and J. Selvaraj, ‘Single-phase seven-level grid-connected inverter for photovoltaic system,” *IEEE Trans. Ind. Electron*., vol. 58, no. 6, pp. 2435–2443, 2011.

[12] O. Husev, C. Roncero-Clemente, E. Romero-Cadaval, D. Vinnikov, and T. Jalakas, “Three-level three-phase quasi-z-source neutral-point-clamped inverter with novel modulation technique for photovoltaic application,” *Electric Power Systems Research*, vol. 130, no. 1, pp. 10-21, 2016.

[13] V. Oleschuk and F. Blaabjerg, “Synchronized scheme of continuous space-vector PWM with the real-time control algorithms,” *Proc. of IEEE Power Electron. Specialists Conf. (PESC’2004)*, pp. 1207-1213, 2004.

[14] V. Sonti, S. Jain, and S. Bhattacharya, “Analysis of the modulation strategy for the minimization of the leakage current in the PV grid-connected cascaded multilevel inverter,” *IEEE Trans. Power Electron*., vol. 32, no. 2, pp. 1156-1169, 2017.

[15] Huu-Cong Vu, Tuyen D. Nguyen, Tae-Won Chun, and Hong-Hee Lee, “New virtual space vector modulation scheme to eliminate common-mode voltage with balanced neutral-point voltage for three-level NPC inverters,” *Proc. of IEEE Int’l Future Energy Electronics Conf. and ECCE Asia (IFEEC 2017 - ECCE Asia)*, pp. 313-318, 2017.